



Molecular intervention of colon cancer and inflammation manifestation by tannin capped biocompatible controlled sized gold nanoparticles from *Terminalia bellirica*: A green strategy for pharmacological drug formulation based on nanotechnology principles

S. Karthick Raja Namasivayam¹ · Gayathri Venkatachalam¹ · R. S. Arvind Bharani¹ · J. Aravind Kumar² · S. Sivasubramanian³

Received: 27 March 2021 / Accepted: 27 July 2021 / Published online: 7 August 2021
© King Abdulaziz City for Science and Technology 2021

Abstract

Among the diverse nanomaterials, gold nanoparticles (AuNps) are utilised for various therapeutic application due to the distinct physical, chemical properties and biocompatibility. Synthesis of gold nanoparticles using plants is the promising route. This method is low cost, eco-friendly and higher biological activities. In this present study, Gold nanoparticles were synthesised from fruit extract of *Terminalia bellirica* fruit extract. Their anticancer and anti-inflammatory activity was evaluated against colorectal cancer cell line (HT29) and TNBS-induced zebrafish model. Highly stable tannin capped gold nanoparticles were synthesised from fruit extract broth of *Terminalia bellirica* rapidly. Structural and functional properties of the synthesised nanoparticles were studied by Fourier transform infrared spectroscopy (FTIR), Field Emission Scanning Electron Microscopy (FESEM) equipped with energy-dispersive atomic X-ray spectroscopy (EDAX) and X-ray diffraction (XRD). All the characterisation studies reveal highly stable, crystalline, phytochemicals, mainly tannin doped, spherical, 28 nm controlled sized gold nanoparticles. The molecular mechanism of anticancer activity was studied by determining cancer markers' expression, which was studied using quantitative real-time polymerase chain reaction (qPCR). Antioxidative enzymes' status and apoptosis changes were also investigated. Synthesised nanoparticles brought a drastic reduction of all the tested cancer markers' expression. Notable changes in antioxidative enzymes' status and a good sign of apoptosis were observed in nanoparticles' treatment. The anti-inflammatory activity was studied against TNBS-induced zebrafish model, which was confirmed by determining inflammatory markers' expression TNF- α , iNOS (induced Nitric Oxide Synthase) and histopathological examination. Nanoparticles' treatment recorded a drastic reduction of inflammatory markers' expression. No marked sign of inflammation was also observed in histopathological analysis of the nanoparticles' treatment group. The present study suggests the possible utilisation of *T. bellirica*-mediated gold nanoparticles as an effective therapeutic agent against a prolonged inflammatory disease that progressively develops into cancer.

Keywords Gold nanoparticles · *Terminalia bellirica* · Colorectal cancer · Anticancer · HT29 · qPCR · Gene expression · Anti-inflammation · Zebrafish

Introduction

In recent years, noble metal nanoparticles particularly, gold nanoparticles (AuNps), have gained more considerations in different fields of science and technology due to their notable physical and chemical properties (Bogireddy et al. 2018). In addition, the advancement of gold-based nanomaterials as core-shell nanoparticles, gold nanocomposites, half and a half has risen as a creative, restorative system for diseases

✉ S. Karthick Raja Namasivayam
biologiask@gmail.com

Extended author information available on the last page of the article

and cancer. Whenever the outside of the nanoparticles is adjusted by practical gatherings or atoms or covered with a slim layer of different materials (with various constituents), they show improved properties contrasted with the non-functionalised uncoated particles (Arachchige et al 2017).

Some of the major advantages of nanoparticles as drug delivery vehicles include targeted delivery of the drug, increase in aqueous solubility of the drug, prevention of drug degradation, sustained drug release, increased drug accumulation in the targeted tumour site, prolonged drug half-life, improved bioavailability and decrease in toxic side effects of the drug, and offering an appropriate form for all routes of administration. Thus, these systems could serve as promising anticancer agents for tumour targeting.

Metal nanoparticles can be synthesised up to 50 nm in size with a large surface area facilitating higher doses of drugs. One of the commonly used metal nanoparticles for an improved anticancer drug delivery system is gold nanoparticles (AuNps). AuNps is easy to synthesise by cheap, reliable and straightforward methods in different size range by simple alterations in parameters (Latha et al. 2018). AuNps have various drug delivery applications due to their notable physicochemical characteristics such as ultra-small size, large surface area to mass ratio, higher surface reactivity. AuNps exhibits surface Plasmon resonance bands responsible for large absorption and scattering cross-sections four to five orders of magnitude greater than conventional dyes (Owaid et al. 2017). In addition, the negative charge on the non-toxic and biocompatible AuNps allows them to be easily functionalised by various biomolecules (Hainfeld et al. 2006).

Size-controlled synthesis of noble metal nanoparticles using biological principles has gained more attention. Biosynthesised nanoparticles from plant bioactive metabolites have additional positive effects by exhibiting antimicrobial, anti-inflammation and modulate fibrogenic cytokines (Bai et al. 2018). Biosynthesis of nanoparticles eliminates the environmental concerns with their chemically synthesised counterparts that may involve hazardous chemicals. Distinct advantages in biosynthesis include enhanced stability, better control over nanoparticle shape and monodispersity (Singh et al. 2015). Most nanoparticles with sizes less than 100 nm have outstanding ability to target tumours, small enough to permeate out from vascular endothelial openings surrounding the tumour region and proved to be non-toxic, biodegradable, preventing systemic side effects by improving the safety and efficacy of sustained drug release (Shang et al. 2018).

In this study, AuNps was biosynthesised by reducing Chloroauric acid with water extract of *Terminalia bellerica*—one of the major component of the polyherbal formulation of Triphala, which is renowned for its various therapeutic uses that include gastro-protective effects,

regulation of gut microbiota, anti-diabetic, antimicrobial, antioxidant, radioprotective, anti-neoplastic and anti-inflammatory (Peterson et al. 2017). *Terminalia bellerica* (Combretaceae), commonly known as Bahera in India, has been used in Ayurveda for its diverse medicinal uses (Sharma et al. 2010). *Terminalia bellerica* is known for its diverse, active medicinal properties such as analgesic (Khan et al. 2008), antimicrobial (Devi et al. 2014), anti-diarrhoeal (Kumar et al. 2010), wound-healing activity (Saha et al. 2011) and anti-ulcer (Choudhary 2012). Potential biological activities of the fruit extract of *Terminalia bellerica* has been revealed by Dharmaratne et al. (2018). The metabolite constituents of the fruit include Tannins, Chebulinic acid, Gallic acid, Glucoside and Ethyl Gallate, which functions as an antioxidant, antimicrobial, antidiarrheal, anticancer, antihypertensive, hepatoprotective and antipyretic agent (Deb et al. 2016). The presence of various phytochemical constituents exhibits a wide range of pharmacotherapeutic activities (Beigi et al. 2018). It can be seen that the diverse phytochemical constituents in the *T. bellerica* are responsible for the synthesis of diverse nanoparticles by acting as bio-reducers or capping agents. These capping agents exhibit diverse pharmacological activities. Hence, *T. bellerica* is selected for the synthesis of diverse nanoparticles via green route principles.

In the present study, gold nanoparticles were synthesised from dried fruit powder extract broth. The synthesised nanoparticles were screened for anti-inflammatory and cancer-targeting effects on the zebrafish model and HT29 colon cancer cells. Prolonged Inflammatory Bowel Disease (IBD), affecting at least one-third of the colon, is extensively acknowledged as one of the most vital risk factors leading to the development of colorectal cancer (CRC), in which dysplasia or intraepithelial neoplasia is the precursor (Singh et al 2017). Colorectal cancer ranks in the highest third of cases reported globally (Khan and Khan 2018). Despite IBD accounting only for 1–2% of CRC in the overall population, IBD patients have the possibility of developing CRC at a younger age with more aggressive multifactorial symptoms expressed at an advanced stage compared to sporadic or familial CRC. These combined factors result in a worse likely course of the medical condition, with one in six IBD patients dying due to CRC. The risk factors involved in CRC occurrence in IBD include the severity of inflammation, extent and age of IBD onset, percentage of colon involved, primary coexistent sclerosing cholangitis and familial CRC history (Hao et al. 2019). Combined genetic and environmental factors such as oxidative stress, epigenetic alteration, genetic instability, intestinal microbiota and mucosal inflammatory-mediated immune response are responsible for neoplasia occurrence in IBD-associated CRC (Marill et al 2019).

Conventional methods to treat CRC involve neoadjuvant chemo- and radiotherapy followed by surgical excision and adjuvant chemotherapy depending on the tumour stage. Chemotherapy has considerable intolerance and failure due to poor localisation of drugs to tumour-specific tissues and systemic side effects. Some cancer cells have inherent resistance towards radiations make them less effective (Chen et al. 2019). Nanotechnology-based principles are now extensively utilised in biomedicine as an anti-inflammatory agent due to the distinct Physico-chemical and biocompatibility properties (Namasivayam et al. 2020). Anticancer activity was confirmed by inhibition in cell viability and proliferation, changes in antioxidative enzymes and gene expression pattern leading to apoptosis activation. Thus, green-synthesised gold nanoparticles prove to be a promising anti-inflammatory and anticancer agent that can prevent IBD and IBD-associated colorectal cancer progression.

Materials and methods

Gold nanoparticles' synthesis (AuNps)

Fruit extract of *Terminalia bellirica* was used for the synthesis of nanoparticles. Dried fruit powder of *T. bellirica* was obtained from siddha medical shop as the commercial formulation. Aqueous extract or plant extract broth was prepared from the collected powder was used as the source for biosynthesis. Known quantity (2.5 g) of powder was suspended in 100 ml of distilled water, boiled in water bath (50 °C) for 2 h followed by filter through Whatman No. 1 filter paper. Collected filtrate was concentrated in rota evaporator Concentrated extract thus obtained was collected in screw cap vial and used for further studies. Qualitative phytochemical analysis of the concentrated extract was studied by the standard screening methods (Deb et al. 2016).

In a typical procedure of nanoparticles synthesis, known volume of extract thus prepared (1 ml) was mixed with 4 ml of 0.1 molar final concentration of metal precursor chlorauric chloride (Sigma) that kept in screw cap vial. Reaction mixture thus obtained was incubated at room temperature (30 °C). Preliminary confirmation of synthesis was done by conversion of reaction mixture into ruby red. After the confirmation, the reaction mixture containing the synthesised nanoparticles were purified from the reaction mixture by centrifugation (10,000 rpm, 30 °C). Collected pellets were washed with deionised water thoroughly to remove non-reactive residues and the washed pellets were lyophilised.

Characterisation

Suitable characterisation methods studied the structural and functional properties of the purified nanoparticles.

Before characterisation studies, the sample was dispersed thoroughly in a suitable dispersion medium followed by sonication. UV–visible absorption spectroscopy study was done to determine surface Plasmon absorption maxima using Shimadzu-1800 spectrophotometer with 800–200 nm range. Functional groups were determined by Fourier transforms infrared spectroscopy (FTIR) analysis with Bruker Optic GmbH Tensor 27 (400–4000 cm^{-1} scanning range). Morphology studies were done with field emission scanning electron microscopy (FESEM). SUPRA 55-CARL ZEISS (magnification range 35–10,000, resolution 200 Å, acceleration voltage 19 kV). Technai F 12. Elemental composition was studied by energy-dispersive atomic X-ray spectroscopy (EDAX) equipped with FESEM.

Further characterisation was done using atomic force microscopy (AFM), which reveals surface topology. Samples were examined with AFM Ntegra Prima-NTMDT, Ireland. The crystalline phase of the nanoparticles was determined by X-ray diffraction (XRD) analysis (Rigaku smart lab—Voltage of 40 kV and a current of 30 mA with Cu K α radiations).

Stability was done by exposing the synthesised nanoparticle suspension at ambient condition. After 30-day exposure, zeta potential was measured using zetasizer (Malvern, UK). Evaluation of colour change and aggregate formation also reveals the notable stability.

Anticancer activity

Anticancer activity was studied against human colorectal cancer Cell Line (HT29) by determining cell viability inhibition, antioxidative enzymes' status and gene expression pattern (qualitative), which triggers apoptosis process.

Cell viability assay

Primary determination of the cytotoxic effect of gold nanoparticles on the HT 29 cells was studied by tetrazolium-based semiautomated colourimetric assay (Carmichael et al. 1987). The cell line was obtained from the National Centre for Cell Sciences (NCCS), Pune, India. The collected cell line was maintained on RPMI media supplemented with 10% foetal calf serum and 1% penicillin–streptomycin solution. Nanoparticles induced toxic effect on the cell line. The optimum condition was provided for the culturing of the cells. After reaching sufficient growth, the cultured cells were exposed to different concentration of nanoparticles, incubated at optimum condition. After the incubation period, the contents were removed completely, fresh medium supplemented with MTT solution (0.5 mg/ml) was added. The seeded plate was incubated at 37 °C for 4 h. During the incubation period, formazan crystal was formed and solubilised by the addition of DMSO. The optical density of the

solubilised mixture was measured at 490 and 630 nm. Three replicates and control were also maintained. Cell viability inhibition rate was determined by measuring the differences in the optical density of the control and treatment group. Nanoparticle-mediated impact on the cell morphological changes was studied by phase-contrast microscopic examination, which reveals the sign of the cytotoxic effect.

Biocompatibility using Vero cell line

Followed by the determination of inhibitory effect, a cell viability assay was done with the Vero cell line to confirm the biocompatibility. Vero is the most commonly employed in vitro model for the toxicity assessment among the various cell cultures due to its fast growth rate and high replication efficacy. As described above, an MTT assay was adopted to study the toxic effect of synthesised nanoparticles with three dosages of synthesised nanoparticles (LC_{50} dosage—49.8, lower LC_{50} —24.9 and higher LC_{50} —74.7 μ g).

Propidium iodide fluorescent staining

Apoptotic changes in the nanoparticles exposed cells were studied by propidium iodide fluorescent staining. This study was divided into four groups—group 1—untreated control, group 2—nanoparticles treated with 25 μ g, group 3—nanoparticles treated with 50 μ g and group 4—nanoparticles treated with 100 μ g. The respective treatment group were washed with phosphate-buffered saline (PBS) followed by fixation with ethanol (70%). Staining of the cells carried out with 0.5 ml of PBS containing 0.01 mg/ml of propidium iodide, incubated in a dark chamber for 30 min at ambient temperature. Stained cells were washed with PBS after the incubation period. Stained cells were examined for the determination of apoptotic changes by the fluorescence microscope with the standard filters.

Antioxidative enzymes' status

Effect of nanoparticles on the major antioxidative enzymes and Lipid peroxidase and glutathione was done by the method of Yuan et al (2017). Glutathione is measured by its reaction with DTNB (5,5'-dithio 2-nitrobenzoic acid) (Ellman's reaction) to give a mixture that absorbs light at 412 nm. 1.8 ml of 0.2 M Na_2HPO_4 was combined with 40 μ L 10 mM DTNB and 160 μ L of cell homogenate (derived from different concentration of extract and gold nanoparticles separately). The blank contained distilled water instead of cell homogenate. It is allowable to stand for 2 min, and the absorbance was read at 412 nm in a UV-Vis spectrophotometer.

Nanoparticle-mediated effect on another major antioxidative enzyme, glutathione S transferase (GST), was also studied. GST catalyses the conjugation of L-glutathione to CDNB through the thiol group of the glutathione. Cell homogenate (derived from Triphala extract, nanoparticles) was mixed with a suitable substrate. The reaction product obtained was measured spectrophotometrically. The reaction product, GS-DNB Conjugate, absorbs at 340 nm. The increase in the absorption is directly proportional to the GST activity in the sample (Uchide et al. 2006).

Followed by GSH, GST, LPO, antioxidative enzymes, measurement of lactate dehydrogenase (LDH)—an oxidoreductase that catalyses the lactate's interconversion pyruvate. LDH is most often measured to assess the presence of tissue or cell damage. The non-radioactive colourimetric LDH assay is based on reducing the tetrazolium salt MTT in an NADH Coupled enzymatic reaction to a decreased form of MTT that shows a maximum absorption peak (OD) at 565 nm. The purple colour concentration is directly proportional to the enzyme activity (Halliwell and Gutteridge 2015).

Nanoparticle-induced changes in the gene expression pattern

The impact of nanoparticles on the gene expression profile of three major genes (β -actin, PRAP and tumour necrosis factor-alpha) was studied by reverse transcriptase quantitative real-time polymerase chain reaction. qPCR was carried out followed by RT-PCR to reveal the expression level quantitatively. Quantitative assessment of PCR-amplified products of each gene reveals the nanoparticle-based impact. The amount of the expressed respective gene reveals nanoparticle-mediated effect. Initially, DNA was extracted from the cell lines treated with LC_{50} dosage of fruit extract and nanoparticles using a DNA extraction kit (Sigma-Aldrich). Nucleotide sequence alignments of β -Actin and PARP genes were obtained through databases. Based on these alignments, primers were designed (Table 1).

Table 1 Primers of selected colon cancer and inflammatory marker genes

Primer sequence	Nucleotide sequences
PARP forward	5'CCCAGCCTTGTGGAAAACAC3'
PARP reverse	5'CACCTGCAGAGACAGGCATT 3'
β -Actin forward	5'TCAAGGTGGGTGTCTTTCCTG3'
β -Actin reverse	5'ATTGCGGTGGACGATGGAG 3'
TNF- α forward	5'ACACAGAAGACACTCAGGGA3'
TNF- α reverse	5'CCGGTACTAACCCTACCCCC 3'
iNOS forward	5'ACACTTCGAAAAGCAAGATGG 3'
iNOS reverse	5'ACGGGCATCGAAAAGCTGTA 3'

In RT-PCR, the total RNA of the respective treatment group was isolated under standard isolation protocol, and the isolated pure RNA was used as the template for cDNA synthesis. Followed by cDNA synthesis, qPCR –ideally used for gene expression analysis which measures relative and absolute amounts of genes with appropriate and reference values. Synthesised cDNA attaches to the fluorescent marker, amplified into millions of copies with the respective colon cancer gene primers. Data were analysed using the comparative c1 method.

Anti-inflammatory activity

Gold nanoparticle-induced anti-inflammatory activity of nanoparticles against the zebrafish model was studied by determining inflammatory markers and histological analysis. The synthesised nanoparticles always need to be tested for their biological effects, such as biocompatibility and cytotoxicity, before applying. Several biological models from mammalian cell lines for in vitro and mice and the Danio rerio (Zebrafish) model for in vivo studies have been employed. Zebrafish models have been established as a promising and effective model to study biological effects due to their short life cycle, economic rearing and higher genetic similarity with humans (Kumari et al. 2019).

Zebrafish collection and maintenance

Adult zebra fishes that are healthy and devoid of any malformations or infections were chosen for the study. Before the initialisation of the experiment, fishes were acclimatised to lab conditions according to OECD guidelines (OECD, 203). Fishes were grouped as a positive control (TNBS + PBS). The treatment group composed of LC₅₀ dosage of fruit extract nanoparticles separately. At the ending of the experiment, fishes were euthanised by decapitation with proper anaesthesia.

LC₅₀ determination

Zebrafishes of interest were weighed. According to their weight, the concentration of the sample to be injected in 20 µL volume was calculated (in PBS, Ph—7.4). 31G Calibre injections were employed in this study. Before injection, a base plane was set to hold the fish; a soft sponge with 1.5 cm cut in the centre, in a box or a Petri dish filled with ice water (12 °C). Test solutions were loaded up in the injection before anaesthesia. Each fish was slowly anaesthetised by adding +ce chips into the fish water until the temperature reaches 12 °C. When the fish remains to any external stimuli, transfer it to the base plane, holding the fish in the sponge with the abdomen facing up. Without delay, injected intrarectally and fishes were

injected into normal water, where fish recovers at once, regaining normal behaviours. From the time of injection, fishes were observed for 10 days (OECD, 203). The number of animals dead in each concentration from 0 to 10 days was noted, and LC₅₀ was determined.

Induction of inflammation with TNBS and efficacy analysis

For testing the efficacy, extract and nanoparticles were injected intraperitoneally at LC₅₀ dosages. TNBS was prepared in the concentration range of 160 mM using 30% ethanol. The fishes were weighed, and TNBC injection was given 1 µL/0.1 g body weight. After 6 h of TNBS induction, drug (Samples) was given and maintained for the treatment period of 10 days. After that, fishes were euthanised to cease the biological reactions at the end of the experiment.

Histology

After 4 h, fishes were decapitated. Their abdomen region was excised and fixed in Dietrich's fixative and transferred for histopathology analysis (source: Zebrafish International Resource centre). The remaining tissues were immediately stored at 4 °C for DNA extraction.

Inflammatory markers' gene expression

Gold nanoparticle-induced effect on the expression of inflammatory markers such as TNF-α and iNOS (induced Nitric Oxide Synthase) was studied by quantitative RT-PCR. Respective gene primers were designed with the NCBI Primer-BLAST tool. The sequences are listed in Table 1. Other than the inflammatory markers employed here, β-actin was taken as the control for the housekeeping gene. Total RNA was isolated from the respective treatment group using a standard protocol. The isolated cellular total RNA was used as the template for the synthesis of cDNA.

The real-time qPCR conditions are followed according to the manufacture instruction as follows: initial denaturation at 95 °C for 10 min, trailed by 45 cycles of 3 step amplification consisting denaturation at 95 °C for 15 s, annealing 60 °C for 15 s and extension at 72 °C for 30 s. The melting curve was analysed from 60 to 95 °C for 20 s. The expression of each target genes has its own (ct) amplification value at the threshold level. The products of the PCR start to detect the fluorescence.

Statistical analysis

All the data were subjected to *t* test models for the determination of statistical significance.

Results and discussion

Among the diverse nanomaterials, gold nanoparticles (AuNPs) play a major role in biomedicine owing to their distinct structural, functional properties, including biocompatibility (Kamal et al. 2018). Synthesis of gold nanoparticles using plants based is quite popular due to the high

efficacy and eco-friendly. In this present investigation, gold nanoparticles (AuNPs) were synthesised from fruit extract of *Terminalia bellirica*. The synthesised nanoparticles were evaluated for the molecular mechanism of anticancer and anti-inflammatory activities. Colorectal cancer cell line (HT29) was selected for the anticancer activities using cell viability antioxidative enzymes' status, apoptosis and gene

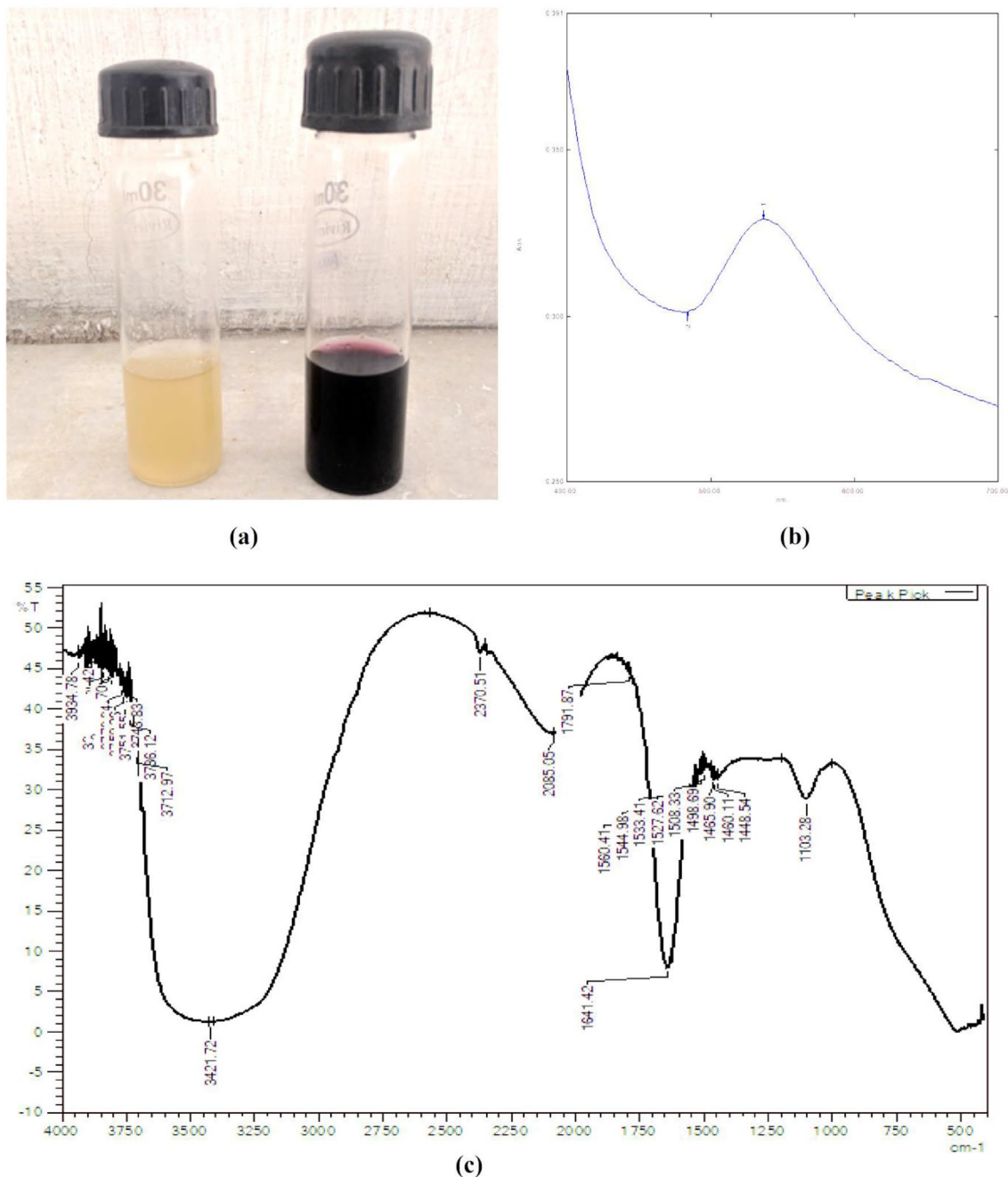


Fig. 1 Characterisation of AuNPs: **a** synthesised AuNPs in the fruit extract broth, **b** UV-visible spectra of the synthesised AuNPs and **c** FTIR spectra of synthesised AuNPs

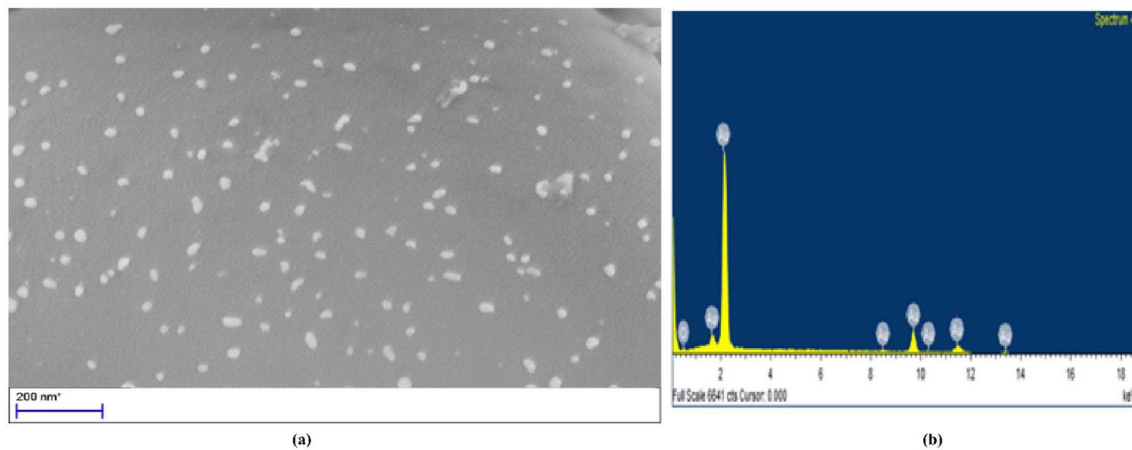


Fig. 2 Characterisation of AuNPs: **a** SEM micrograph, **b** EDAX spectra

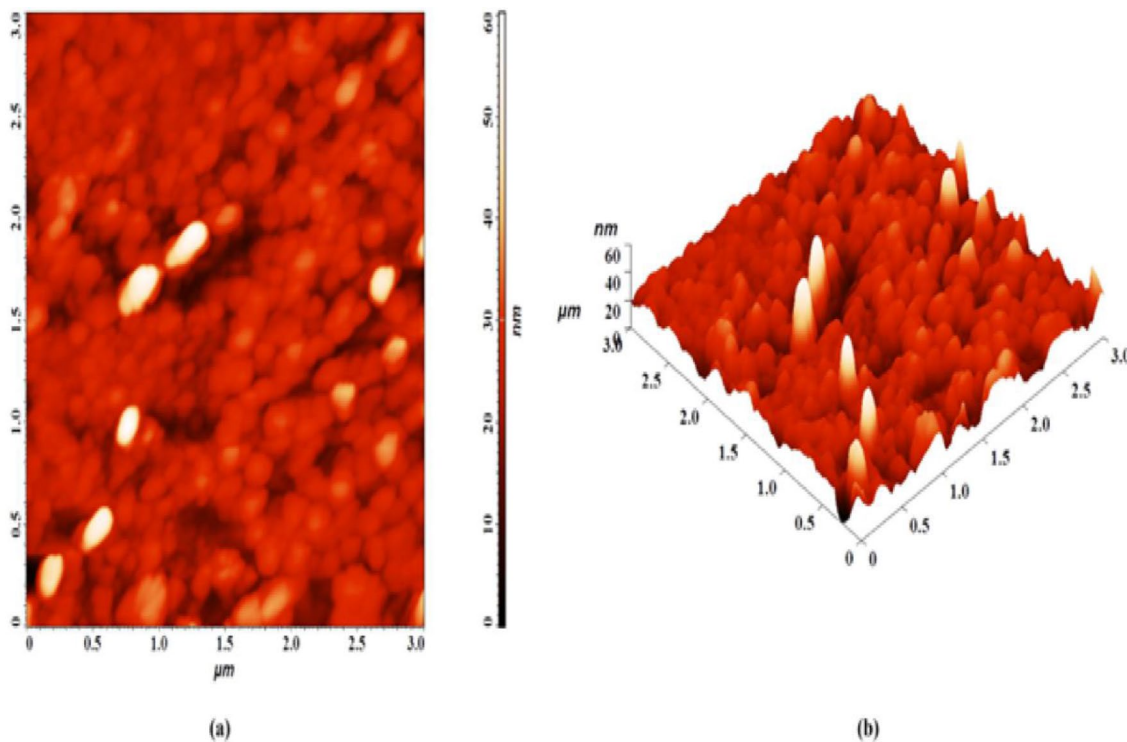


Fig. 3 Characterisation of AuNPs: **a** AFM micrograph-2D, **b** AFM micrograph-3D

expression pattern. TNBS-induced zebrafish was selected for the determination of anti-inflammatory activity.

Phytochemical analysis

Terminalia bellirica aqueous extract prepared for the biosynthesis was evaluated for phytochemical analysis. Aqueous fruit extract prepared from *Terminalia bellirica* was tested qualitatively to determine the presence of various bioactive

phytoconstituents. The analysis results show various bioactive phytochemical constituents such as alkaloids, flavonoids, phenolics and tannins. Hazra (2019) reported the phytochemical screening of various parts of *Terminalia bellirica* fruits in the aqueous extract. A variety of phytochemicals present in the plant extracts are non-nutrient compound possessing biological activity that can be of valuable therapeutic index. Diverse phytochemicals have been found to possess a wide range of activities, which may help in protection against chronic diseases.

Fig. 4 Characterisation of AuNps—XRD pattern of synthesised AuNps

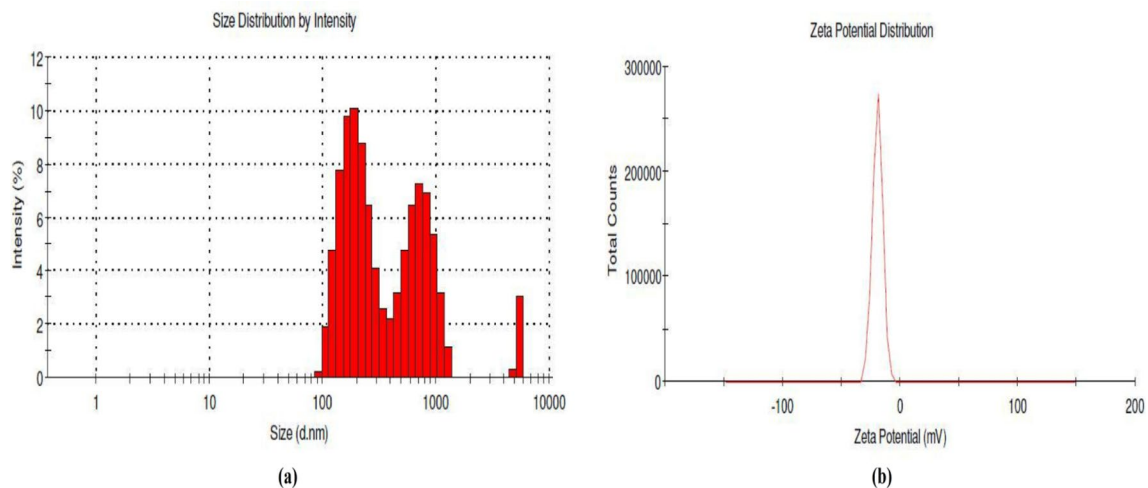
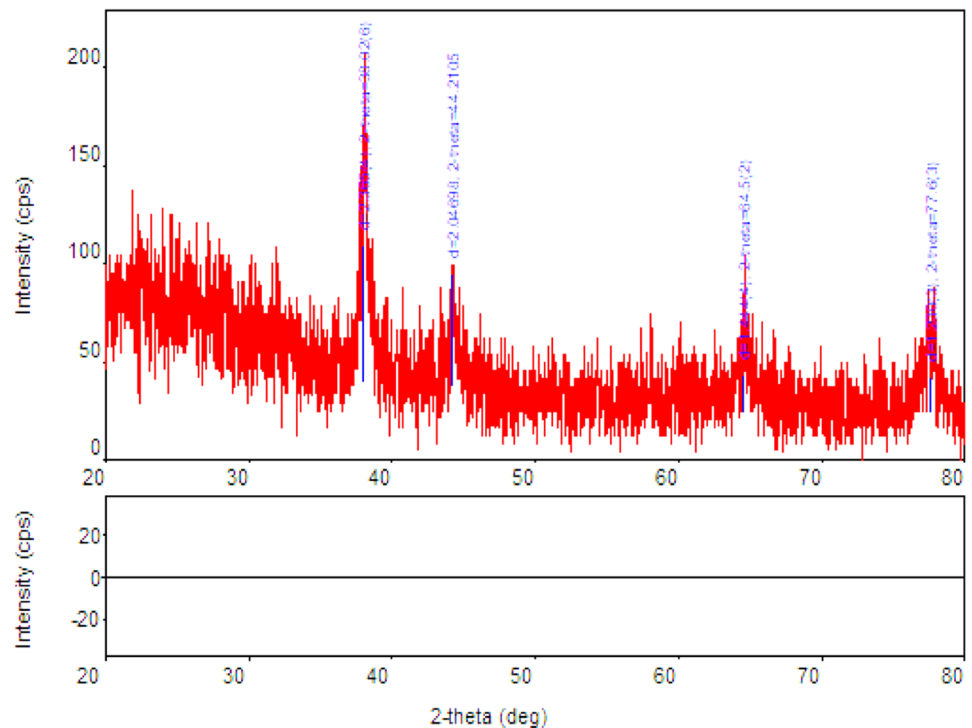


Fig. 5 Zeta potential (mV) of synthesised AuNps

Synthesis of gold nanoparticles (AuNps)

Biosynthesis of AuNps was affirmed by the conversion of reaction mixture into trademark ruby red rapidly at 5–10 min. (Fig. 1a). The oscillation of free conduction electrons incited by an associating electromagnetic field is liable for the colour change. Essential affirmation was done by UV–visible spectroscopy examines which demonstrate that a sharp plasmon peak at 545 nm associated with a striking peak at 270 nm, which uncovers the nearness of tannins—a

significant phytochemical responsible for bioreduction (Fig. 1b). The characterisation was additionally examined by FTIR examination, which is utilised to investigate the functional groups. FTIR spectra show the wavenumbers which specific to essential amine, alkyl, ketone or carboxylic groups. Particles' morphology study by scanning electron microscopy (SEM) equipped with energy-dispersive atomic X-ray spectroscopy (EDAX) shows that the particles are monodisperse, non-agglomerated spherical shape with the size of 28 nm (Fig. 2) and various factors

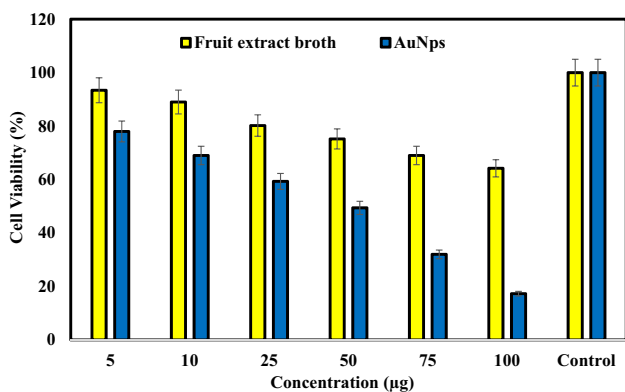


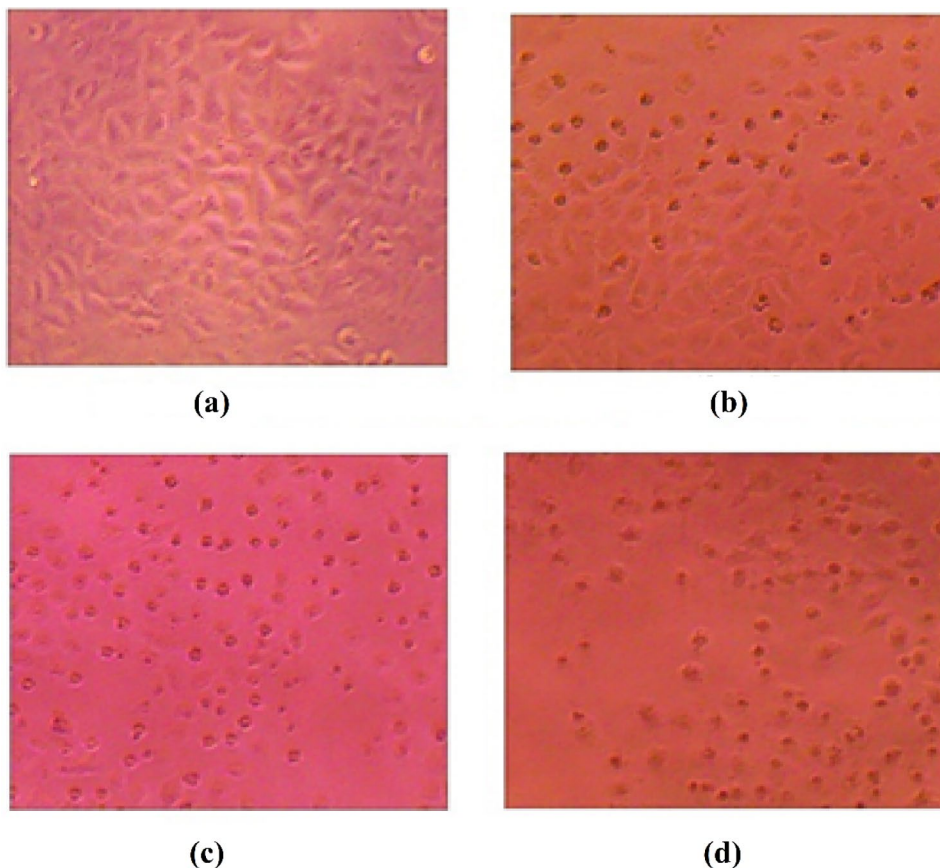
Fig. 6 Cell viability (%) of HT29 cells

govern the synthesis of nanoparticles with the controlled size. Synthesis of nanoparticles with the controlled size and shape by physical and chemical methods has been reported earlier. However, biological principles for the synthesis of nanoparticles with controlled size are limited. A study by Bogireddy et al. (2018) reported that the gold nanoparticles with the controlled size were synthesised from an aqueous extract of *Coffea Arabica*. Their finding revealed that the pH of the aqueous extract of *Coffea Arabica* acts as the factor

for synthesising gold nanoparticles with the controlled size. Our present study, an aqueous extract of *Terminalia bellirica*, brought about gold nanoparticles with the controlled size and shape. Phytochemical constituents in the aqueous extract of *T. bellirica* seems to be reducing and capping agent for the growth of AuNps. It may be hypothesised that the various phytochemicals and the pH of the extract act as the determinative factor for the controlled size and shape of the nanoparticles. Elemental composition was studied by EDAX analysis equipped with SEM. EDAX spectra of the synthesised gold nanoparticles are displayed in Fig. 2b. A notable sign from the incorporated gold nanoparticles (60.0% in mass) was recorded. A more fragile sign from C and O was also observed, which affirms bio-reducer. AFM is a significant characterisation technique for the assurance of disintegration and agglomeration as an example of synthesised nanoparticles. The geographical picture of gold nanoparticles, specifically brilliant spots, demonstrates the shaped nanoparticles all around appropriated with the normal size of 28 nm (Fig. 3).

Further characterisation of synthesised AuNps was done by XRD investigation, which is utilised to decide the nanoparticles' shape, size and basic physical security. The XRD pattern is shown in Fig. 4, which uncovers distinct diffraction peak in the entire range of 2 θ values, going from 20 to

Fig. 7 Phase-contrast microscopic examination of HT29 cells: a control, b 25 µg, c 50 µg and d 100 µg



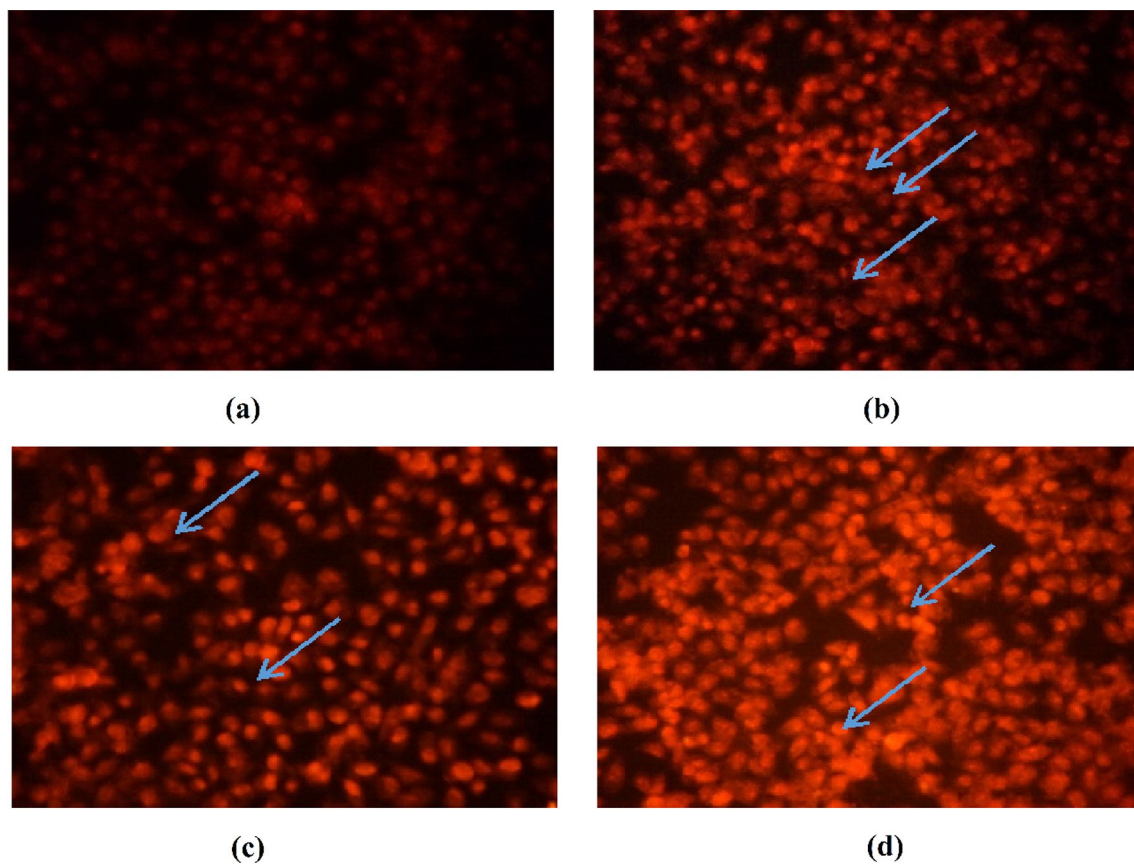


Fig. 8 Propidium iodide staining of HT29 cells: **a** control, **b** 25 μg , **c** 50 μg and **d** 100 μg

80. XRD spectra of unadulterated crystalline gold structures have been distributed by the Joint Committee on Powder Diffraction Standards (record nos.04–0784). A correlation of our XRD range with the standard example affirmed that the gold nanoparticles had been framed as crystalline. A strong peak at 2 θ estimations of 38.21, 44.44, 64.61 and 77.63 relating to (111), (200), (220) and (311) arrangement of planes for gold nanoparticles which demonstrates that crystalline nature of the readied AuNps.

Stability of the synthesised nanoparticles was done by zeta potential which is the important parameter which influences their stability in suspension. Zeta potential-recorded after 30 days after storage. Zetasizer (Malvern, UK) was used to determine zeta potential, particle size distribution, which reveals well-distributed particles with a size range of 204.1 nm dia. Zeta potential is the important parameter which influences their stability in suspension. Zeta potential value of the nanocomposite was in negative range -14.6 mV and -19.1 mV (Fig. 5). The mutual repulsion of nanoparticles depends on having either a significant negative or positive zeta potential. Zeta potential of the nanoparticles in the negative range indicates high stability, colloidal nature and high disparity.

Anticancer activity

Anticancer activity of gold nanoparticles was examined against human colon cancer cell line HT29 by determining cell viability, antioxidative enzyme profile, the qualitative expression profile of β -actin, PRAP and tumour necrosis factor-alpha (TNF- α). Figure 6 portrays the cell viability rate (%) of gold nanoparticles against HT 29 cell line adopting MTT assay. All the tested concentration of nanoparticles restrained the cell viability. A continuous increase in cell viability was recorded in higher dosages (Fig. 6). A compelling anticancer activity was likewise affirmed by LC_{50} . Lower LC_{50} demonstrates the most elevated restraint action. Gold nanoparticles recorded LC_{50} at 49.2 μg also reveals an enhanced anticancer activity. Microscopic examination using phase-contrast microscopy shows the cytotoxic effect of nanoparticles which was inferred from Fig. 7. Notable changes in cell morphology, including cell number, were observed in nanoparticles exposed cells. Nanoparticle-induced toxic effect was confirmed by the characteristic changes in cellular architecture such as cell fragmentation, more cellular abnormalities, aggressive with cytoplasmic condensation and membrane integrity changes.

Table 2 A comparison of previously reported nanomaterials with AuNPs that synthesised in the present system-based anticancer and anti-inflammatory activities

S. no.	Nanomaterial	Parameters tested	Gold nanoparticles synthesised in the present study
	Anticancer activity		
1	Polydopamine-coated Au–Ag nanoparticles (Hao et al. 2019)	Chemical route of synthesis, Photothermal therapy adopted No report on anti-inflammatory activity	Biologically synthesised gold nanoparticles Cell viability assay, antioxidative enzyme profile, LDH release and apoptosis Gene expression studies Anti-inflammatory activity was also investigated using zebrafish model
2	Deoxycholic acid and hydroxybutyl decorated chitosan nanoparticles (DAHBC NPs) as oral curcumin (CUR) delivery system (Wang et al. 2019a, b)	Drug loading efficacy and biocompatibility No report on anti-inflammatory activity	Green synthesis route Recorded cytotoxic effect at lower concentration, notable changes in antioxidative enzymes Anti-inflammatory activity was also investigated using zebrafish model
3	Tio-GNPs (Shi et al. 2016)	Anti-tumour activity of chemically synthesised Tio-GNPs using animal model sensitised with X-rays In vitro toxicity using HT 29 cell line No report on gene expression pattern, antioxidative enzymes' status Anti-inflammatory activity using zebrafish model	Biologically synthesised nanoparticles In vitro cell line model system was used to check the anticancer activity without the use of radioactivity studies Changes in antioxidative enzymes, gene expression profile and apoptosis studies Anti-inflammatory activity was also investigated using zebrafish model
4	Hafnium oxide Nanoparticles that activated with radioactivity (Zhang et al. 2020)	Radiotherapy-activated hafnium oxide Nanoparticles and its anticancer activity on mouse model—immunohistochemistry and digital pathology analysis	Biologically synthesised gold nanoparticles Cell viability assay, antioxidative enzymes' profile, LDH release and apoptosis Gene expression studies Anti-inflammatory activity was also investigated using zebrafish model
5	Paclitaxel-loaded PLGA nanoparticles (Zhong et al. 2019)	Paclitaxel release study, cell cycle and apoptosis assay	Exhibited notable cytotoxic effect without any anticancer agents conjugation Anti-inflammatory activity against zebrafish model
6	Radiotherapy-activated hafnium oxide nanoparticles (Marill et al. 2019)	Activation of the cGAS-STING pathway, cell death, DNA damage	Without radioactivity treatment, synthesised gold nanoparticles shows notable anticancer activity Anti-inflammatory activity against zebrafish model
7	5-Fluorouracil by epigallocatechin-3-gallate co-loaded in wheat germ agglutinin-conjugated nanoparticles (Wang et al. 2019a, b)	Release profile studies, apoptosis detection, cell cycle analysis, biodistribution and pharmacokinetics activities No report on anti-inflammatory activity	No drug loading with the synthesised gold nanoparticles Notable cytotoxic effect on the tested cancer line Recorded an inflammatory activity against zebrafish-induced model
8	Silver nanoparticles decorated with Graphene as radiosensitisers (Habiba et al. 2019)	Anticancer efficacy using animal model and colorectal cancer cell line No report on anti-inflammatory activity	Green-synthesised gold nanoparticles without any drug or added stabilisers exhibited anticancer activity. Anti-inflammatory activity also recorded
9	<i>Camellia sinensis</i> -mediated silver nanoparticles	Cell viability assay. No report on antioxidative enzymes' status, gene expression profile and apoptosis studies, anti-inflammatory activity	Biologically synthesised gold nanoparticles Cell viability assay, antioxidative enzymes' profile, LDH release and apoptosis Gene expression studies Anti-inflammatory activity was also investigated using zebrafish model

Table 2 (continued)

S. no.	Nanomaterial	Parameters tested	Gold nanoparticles synthesised in the present study
10	<i>Murraya koenigii</i> leaf extract-based silver nanoparticles (Roshni et al. 2018)	Cell viability assay No report on antioxidative enzymes' status, gene expression profile and apoptosis studies, anti-inflammatory activity	Biologically synthesised gold nanoparticles Cell viability assay, antioxidative enzymes' profile, LDH release and apoptosis Gene expression studies Anti-inflammatory activity was also investigated using zebrafish model
11	Anti-inflammatory activity IA novel gold glyconanoparticles coating with DS disaccharide analog	Anti-inflammatory activity against carrageenan-induced paw oedema in a rat model	Green-synthesised gold nanoparticles from <i>Terminalia belitrica</i> Anti-inflammatory against TNBS-incited zebrafish model by determination of inflammatory markers and histopathological evaluation Nanoparticles revealed notable inhibition of inflammatory markers No marked effect on the tissue architecture or tissue damage Green-synthesised nanoparticles inhibited the major inflammatory markers' expression in the zebrafish model No sign of inflammatory cell infiltration Zebrafish model using green-synthesised gold nanoparticles Exhibited drastic reduction of inflammatory markers. No sign of inflammatory cell infiltration
12	Peptide-gold nanoparticle hybrids (Yang et al. 2016)	Anti-inflammatory activity in the peripheral human mononuclear model Immunomodulatory activity using animal model In vitro cell culture using THP-1 cells system and in vivo model	Green synthesised gold nanoparticles using zebrafish model—no sign of inflammation Green synthesised gold nanoparticles tested against zebrafish inflammation-induced model Shows marked inhibition of inflammatory marker genes and inflammatory cells
13	Size-dependent anti-inflammatory activity of peptide gold nanoparticles hybrid (Gao et al. 2019a, b)	Wistar albino rat arthritis model studies NF- κ B pathways by suppressing COX-2 activity	Inflammation-induced zebrafish model by determination of inflammatory marker genes and inflammatory cell infiltration pattern
14	Chemically synthesised gold nanoparticles (Khan and Khan 2018)	Studied using ethanol exposed SH-SY5Y cells—cellular intake of AuNp, cell viability, lactate dehydrogenase assay, apoptosis and necrosis	Inflammation-induced zebrafish model by determination of inflammatory marker genes and inflammatory cell infiltration pattern
15	Plant-mediated gold nanoparticles (Singh 2017)	The cytotoxic effects of AuNP bioconjugates on the vascular system were evaluated using circulating human leukocytes and erythrocytes and HUVEC. Human mononuclear (PBMC) and polymorphonuclear (PMN) cells	Inflammation-induced zebrafish model by determination of inflammatory marker genes and inflammatory cell infiltration pattern
16	Fruit extract of <i>Prunus serrulata</i> : mediated silver and gold nanoparticles (Singh et al. 2017)	Anti-inflammatory activity through inhibition of downstream NF- κ B activation in macrophages (RAW264.7)	Eco-friendly route of gold nanoparticle-mediated anti-inflammatory activity against zebrafish model
17	Peptide-gold nanoparticle hybrids (Gao et al. 2019a, b)	Inhibition of Toll-like receptor 4 (TLR 4) signal transduction pathway in mice model	Notable reduction of inflammatory markers' expression and histopathological analysis
18	Gold nanoparticles—CO releasing molecule complex (Fernandes et al. 2020)	Rapid cell uptake and increase of CO releasing molecules against suitable model	Inflammation-induced zebrafish model by determination of inflammatory marker genes and inflammatory cell infiltration pattern

Further morphological changes such as apoptosis were investigated by propidium oxide fluorescence staining. A good sign of apoptosis was observed in nanoparticle-treated HT 29 cells. The fluorescent micrograph depicted in Fig. 8 shows highly condensed and fragmented nuclear material. Table 2 shows a comparative analysis of diverse nanomaterials with the gold nanoparticles synthesised in the present study. These findings indicate the noteworthy effect of synthesised gold nanoparticles from the aqueous extract of *T. bellirica* against the HT29 cell line by recording a high rate of cell toxicity and a good sign of apoptosis at the least concentration.

Nanoparticle-intervened impact on the antioxidative enzymes such as lipid peroxidase (LPD), reduced glutathione (GSH) and glutathione S transferase (GST) was carried out in this study. Assessment of stress enzymes is a noteworthy parameter for the lethality evaluation. Oxidative stress, which is because of the lopsidedness of reactive oxygen species (ROS), is a basic factor that intercedes the change of sound cells into cancerous cells or the advancement of different maladies. In this present investigation, both the tried doses of plant concentrate and nanoparticles achieved extraordinary changes in the degree of oxidative catalysts. Lipid peroxidase (LPO) level was seen as raised in both fruit extract broth and nanoparticle treatment. A notable rise in LPO was seen in AuNps' treatment (Fig. 9). LPO assumes a huge job in the appearance of oxidative harm brought about by receptive oxygen species. Among the diverse treatment, AuNps' treatment uncovers a noteworthy decrease in GSH and GST levels (Figs. 10 and 11). This investigation demonstrates outstanding oxidative stress initiated by the nanoparticles against tried cancer line.

The nanoparticle-mediated impact on lactate dehydrogenase (LDH) was also considered, and the results were recorded as LDH release. Assurance of LDH release is a significant parameter for the affirmation of apoptosis, cytotoxicity and the degree of intracellular LDH changes the permeability of the cell membrane. In this present examination, trademark changes in the LDH release were recorded (Fig. 12). AuNps' treatment brought about a notable impact on LDH discharge. Nanoparticles with all the dosages showed higher LDH release than fruit extract broth. Impact of various nanoparticles (Iron oxide-chitosan nanocomposite, silver nanoparticle-loaded gemcitabine) on LDH release of different cancer cell line model against different cancer cell line models have bolstered our present finding (Rabel et al. 2019).

Active principles of nanoparticles against the tested colon cell line were additionally affirmed by examining the expression of colon cancer markers TNF- α and PARP. The impact of synthesised AuNps on the respective marker gene was analysed by real-time quantitative polymerase chain

reaction (RT-PCR). qPCR—quantitative real-time PCR was done followed by RT-PCR which is used to determine gene expression level quantitatively. LC₅₀ dosage of fruit extract broth and synthesised gold nanoparticles on the respective marker gene expression level was quantified. Total RNA was isolated from the respective treatment groups. The isolated pure RNA was used as a template for cDNA synthesis with reverse transcriptase quantitative real-time polymerase chain reaction. Synthesised cDNA attaches to the fluorescent marker, amplified into millions of copies with the respective gene primers. Data were analysed using the comparative c1 method. Figure 13 depicts the cDNA expression pattern of the respective treatment group, including control. Thick, sharp DNA bands recorded in the control group were easily differentiated from the treatment groups by showing light, thin bands.

The impact of AuNps on the expression of the respective marker gene is presented in Fig. 14. AuNps' treatment brought about a drastic reduction of TNF-alpha and PRAP gene expression. Results indicate that the expression level was significantly lower than the fruit extract broth and control ($P > 0.05\%$). Several cell death pathways, including apoptosis, necrosis and autophagy, are activated in disease states, including cancer (Marill et al 2019). High levels of tumour-associated calcium signal transduction protein (TROP)-2 have been demonstrated to be strongly associated with tumour necrosis factor (TNF)- α levels in colon cancer (Zhong et al. 2019). Notable reduction of relative gene expression of TNF- α in AuNps' treatment recorded in this study reveals that the tested AuNps triggers the inhibition of the molecular mechanism of cancer progression. PRAP1, a novel gene encoding proline-rich acidic protein 1 (PRAP1), is a p53-responsive gene induced by genotoxic stress (Huang et al. 2012). The level of expression of PRAP determines the progression of cancer. Notable changes in the PRAP gene expression recorded in this study reveal that the synthesised AuNps brought about a marked interruption of cancer progression.

Biocompatibility using Vero cell line

Cell viability of synthesised nanoparticles on the Vero cell line was carried out to determine biocompatibility. Vero is the most commonly employed in vitro model for the toxicity assessment among the various cell cultures due to its fast growth rate and high replication efficacy. Vero cells exposed to three different dosages of synthesised nanoparticles (LC₅₀ dosage, lower LC₅₀ and higher LC₅₀), followed by measuring the cell viability adopting MTT assay. Results indicate that tested nanoparticles with all the tested dosages were not inducing any cytotoxic effect. As in the control group, nanoparticles with all the dosages reveal no effect on cell viability (Fig. 15). No changes in morphological characteristics of the

Fig. 9 Lipid peroxidase (LPO) activity of HT29 cells

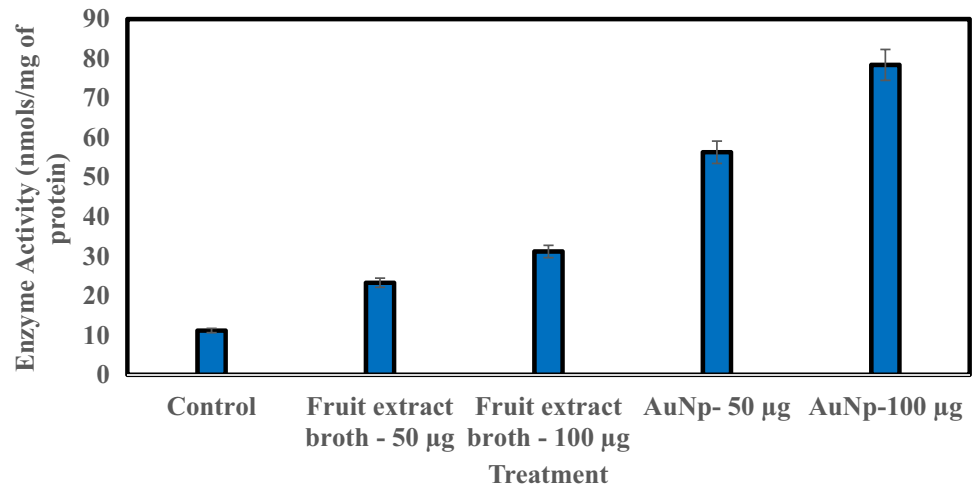


Fig. 10 Reduced glutathione (GSH) activity of HT29 cells

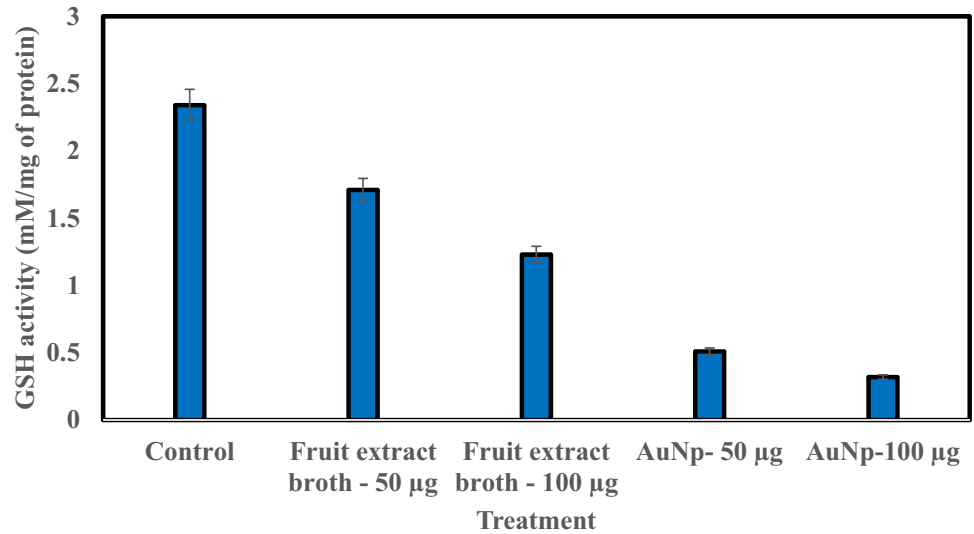
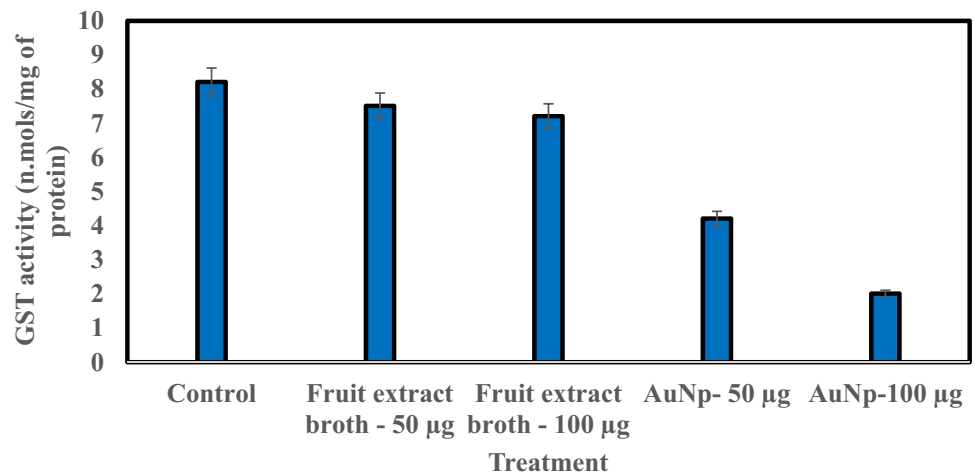


Fig. 11 Glutathione S transferase (GST) activity of HT29 cells



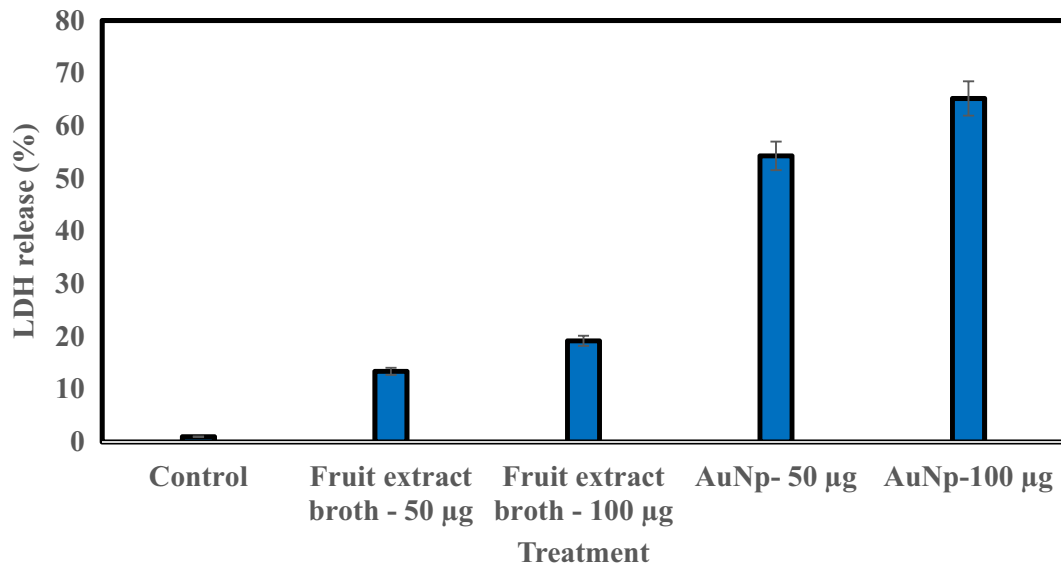


Fig. 12 Lactate dehydrogenase (LDH) activity of HT29 cells

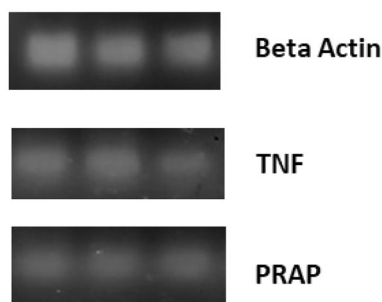


Fig. 13 PCR-amplified products of marker genes. Lane 1—control, Lane 2—fruit extract broth, Lane 3—AuNps

tested cells that were analysed by microscopic examination such as cell count reduction, cell shrinkage, cell lysis, fragmentation or other undesirable abnormalities also confirm the best biocompatibility (Fig. 16).

Anti-inflammatory activity

The anti-inflammatory action of nanoparticles against the zebrafish model was considered by assuring inflammatory markers and histological examination. After the inflammation induction with TNBS in the zebrafish model, synthesised nanoparticles were administrated. After the treatment,

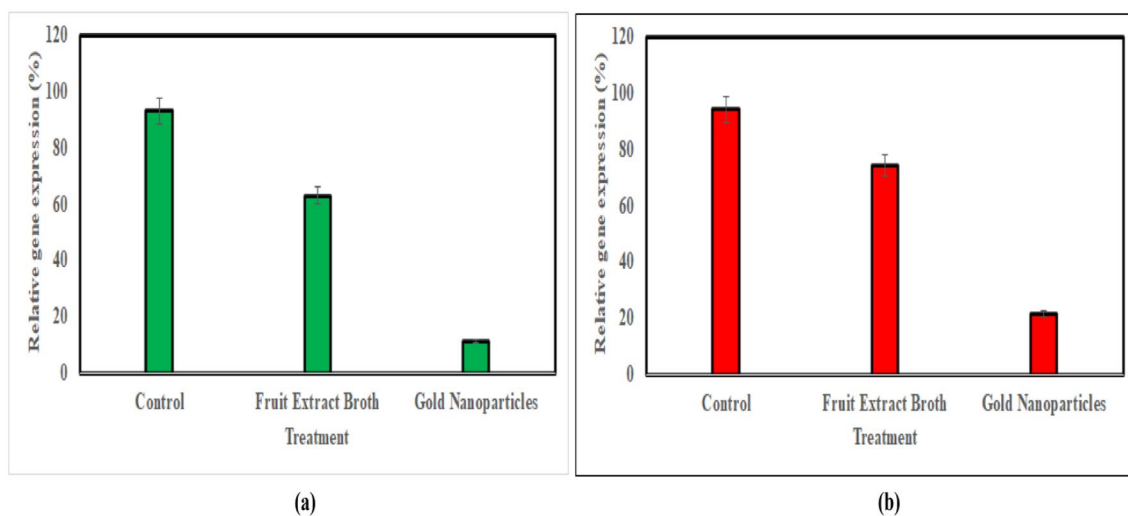


Fig. 14 Relative expression profile of colon cancer marker genes: a TNF-alpha, b PRAP

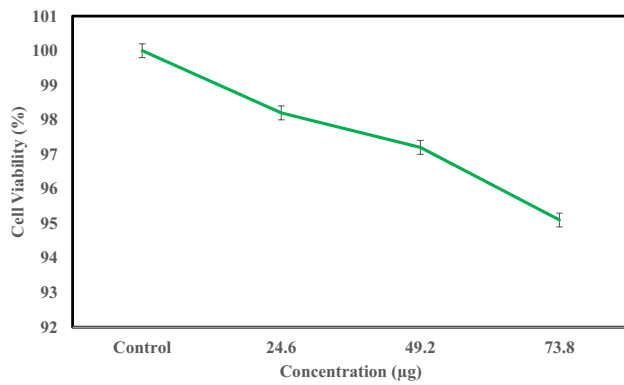


Fig. 15 Cell viability

the tested zebrafish were assessed for inflammatory markers and histopathological examination. RT-PCR determined quantitative inflammatory markers' expression—TNF- α and iNOS (actuated Nitric Oxide Synthase). Total RNA of the respective treatment group was transcribed to cDNA followed by qPCR. qPCR widely used for gene expression analysis measures relative and absolute amounts of genes with appropriate and reference values. cDNA bands shown in Fig. 17 indicate the nanoparticle-mediated impact. cDNA bands observed in control were sharp and thick compared to the thin, low expressed bands in the nanoparticles' treatment group. The relative gene expression rate presented in Fig. 18 reveals that both the fruit extract broth and the orchestrated AuNps recorded changes in all the tried inflammatory markers' expression. A significant effect on the expression was observed in nanoparticle' treatment ($P > 0.05\%$).

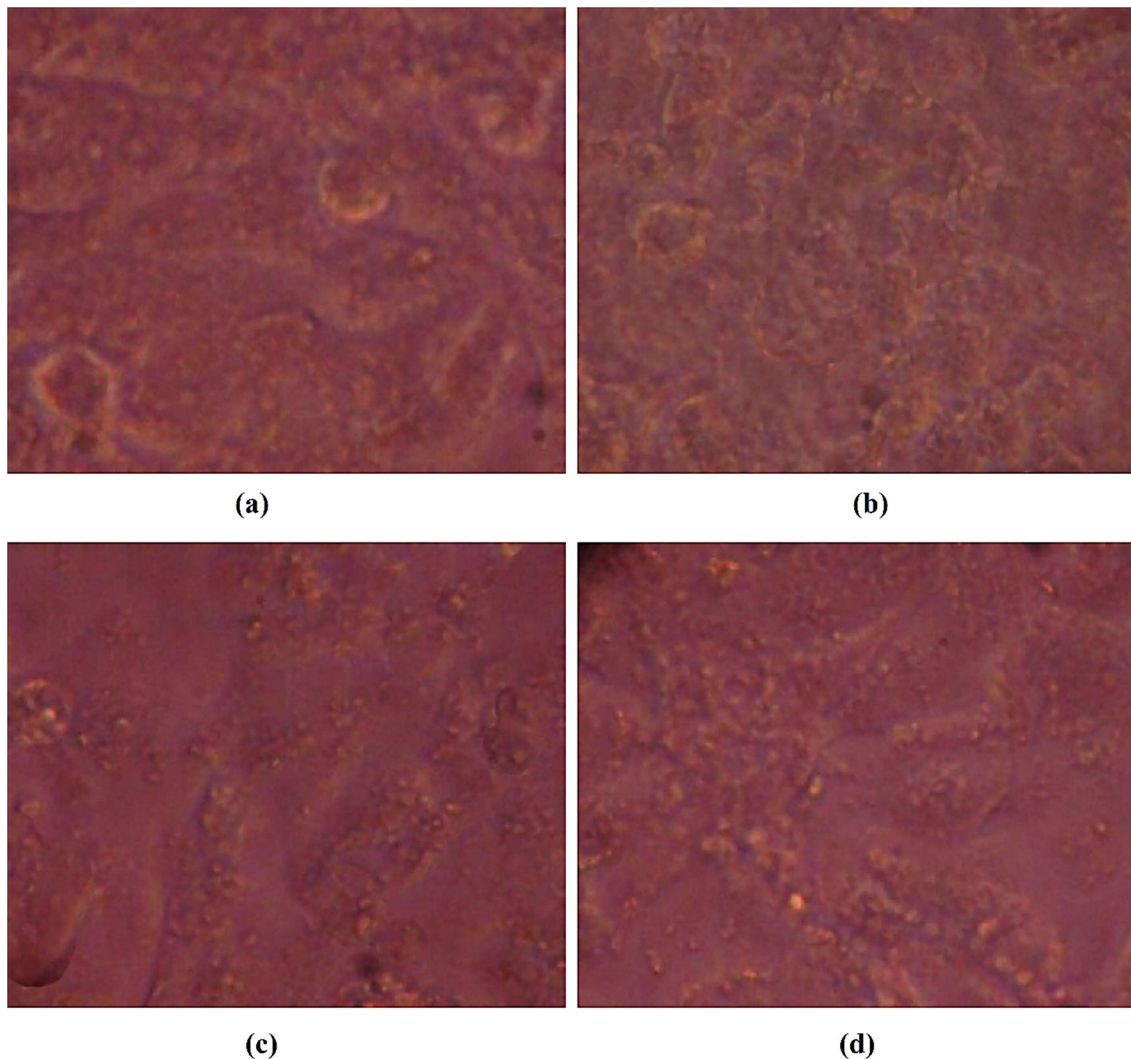


Fig. 16 Microscopic examination of AuNps on Vero cells

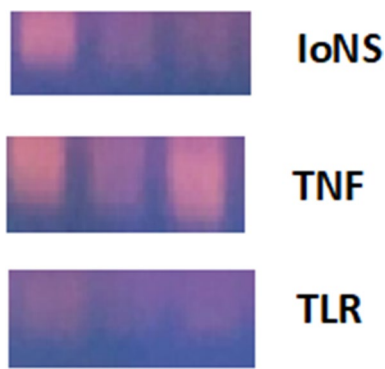


Fig. 17 cDNA of inflammatory marker genes. Lane 1—control, Lane 2—fruit extract broth, Lane 3—AuNPs

Further affirmation of the anti-inflammatory activity of AuNps was done by histopathological assessment of intestinal tissues of the TNBS-incited zebrafish model. Improved decrease of inflammation was seen in AuNp-administrated treatment groups. The degree of decrease was seen as high in AuNps' treatment at the respective incubation period

(Fig. 19). Histopathological assessment of positive control shows that the movement of inflammatory cells (neutrophil) to the inflammation site. Tissue segments from the tested zebrafish of AuNps' treatment demonstrate no unmistakable tissue structure changes or damage signs. A noteworthy sign of aggravation as the relocation of inflammatory cells or neutrophil to the inflammation site was not recorded in the AuNps' treatment groups.

All these results that obtained in this study clearly reveal the biogenic gold nanoparticle-mediated effect on the molecular mechanism of colon cancer and inflammation manifestation. Table 2 shows the comparison of diverse nanomaterials with the gold nanoparticles that are synthesised in the present system-based anticancer and anti-inflammatory activity. From these data, it is very clear that the synthesised nanoparticles showed prominent anticancer anti-inflammatory action by recording noteworthy changes in the gene expression pattern of suitable model system.

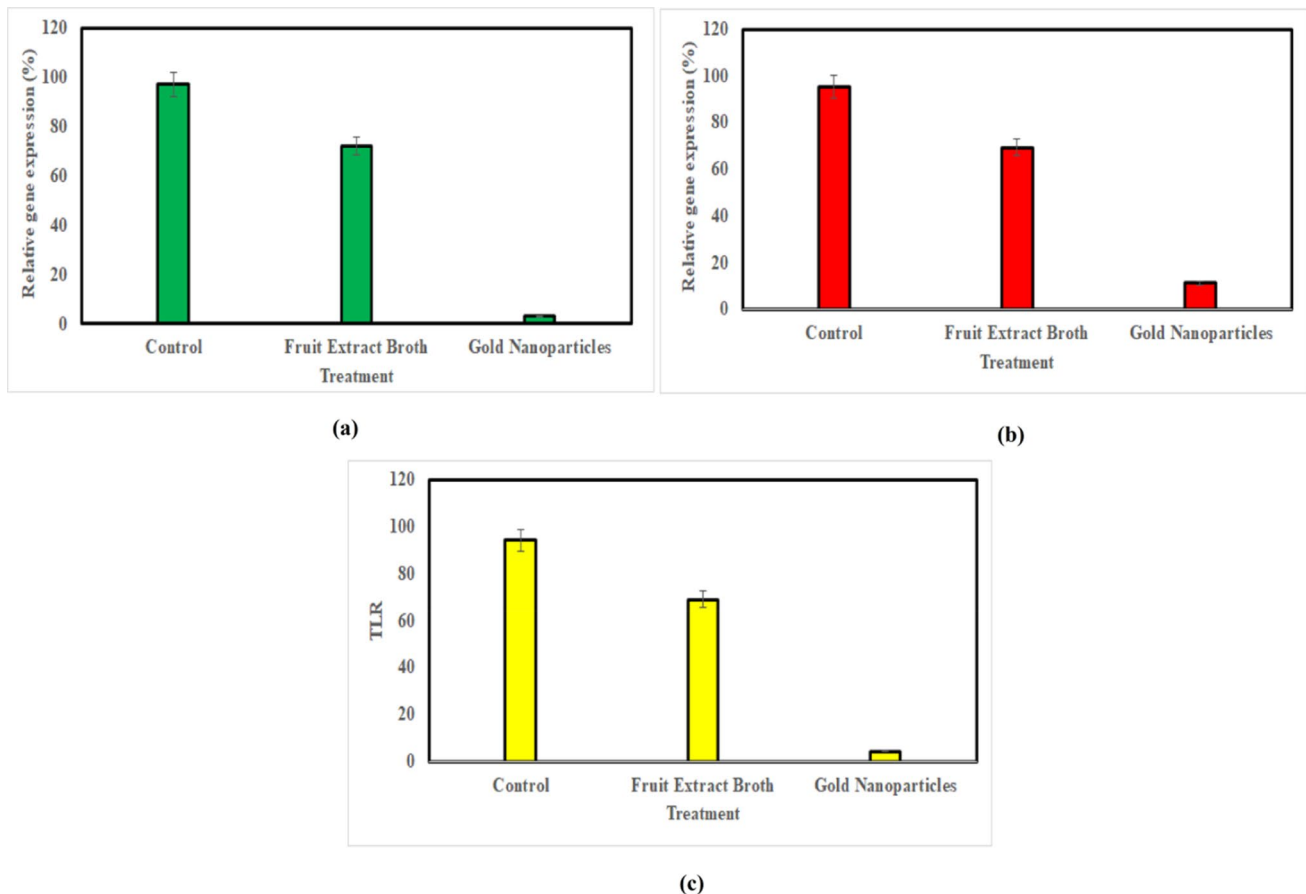


Fig. 18 Relative expression profile of inflammatory markers: **a** TNF-alpha, **b** iNOS

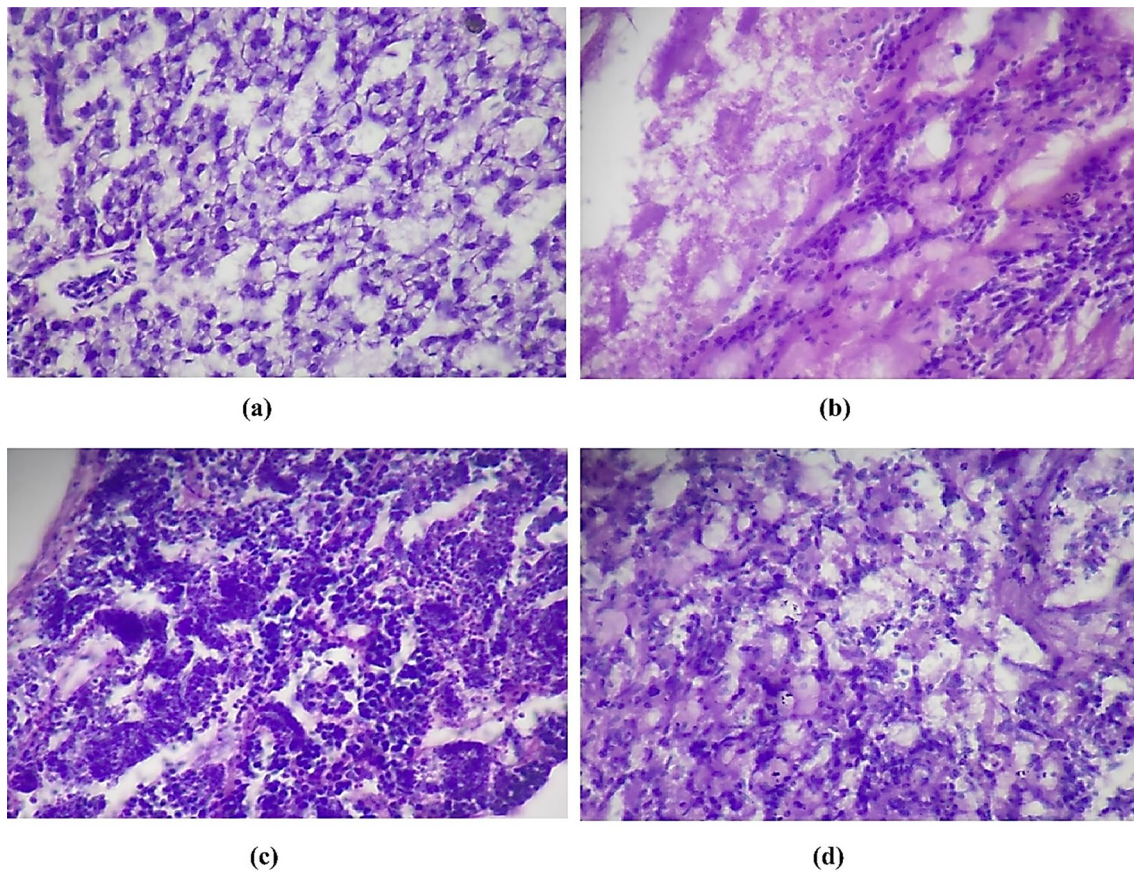


Fig. 19 Histopathological examination of zebrafish model intestinal tissue: **a** control, **b** TNBS induced, **c** fruit extract broth, **d** AuNps

Conclusion

Due to the high efficacy and biocompatibility, gold nanoparticles have numerous applications in the biomedical field. In this present examination, profoundly stable AuNps with the controlled size were synthesised from *T. bellirica* and the synthesised nanoparticles achieved a high pace of anticancer activity against human colorectal cancer cell line (HT29) by recording high cell viability inhibition, prominent changes in antioxidative enzymes and marker genes. Synthesised AuNps also exhibited marked anti-inflammatory action, which was tried utilising TNBS-incited zebrafish model by recording changes in expression of inflammatory markers and histological parameters. Further examinations with an animal model will be helpful to exploit the principles of *T. bellirica*-initiated AuNps as an eco-friendly, biocompatible pharmacological agent.

Data availability

The datasets generated during and/or analysed during the current study are available from the corresponding author on reasonable request.

Acknowledgements We acknowledge SAIF, IIT Madras, India, for the characterisation study of the nanoparticles.

Author contributions Equally contributed.

Funding This research work did not get specific funding from the funding offices in general society, business, or not-revenue-driven sector.

Code availability Not applicable to this study.

Declarations

Conflict of interest We declare that no conflicts of interest.

Ethical approval Not applicable to this study.

Consent to participate Not applicable to this study.

Consent for publication Not applicable to this study.

References

- Arachchige MP, Laha SS, Naik AR et al (2017) Functionalized nanoparticles enable tracking the rapid entry and release of doxorubicin in human pancreatic cancer cells. *Micron* 92:25–31. <https://doi.org/10.1016/j.micron.2016.10.005>
- Bai Aswathanarayan J, Rai Vittal R, Muddegowda U (2018) Anticancer activity of metal nanoparticles and their peptide conjugates against human colon adenorectal carcinoma cells. *Artif Cells, Nanomedicine Biotechnol* 46:1444–1451. <https://doi.org/10.1080/21691401.2017.1373655>
- Beigi M, Haghani E, Alizadeh A, Samani ZN (2018) The pharmacological properties of several species of terminalia in the world. *Int J Pharm Sci Res* 9(10):4079–4088
- Bogireddy NKR, Pal U, Gomez LM, Agarwal V (2018) Size controlled green synthesis of gold nanoparticles using *Coffea arabica* seed extract and their catalytic performance in 4-nitrophenol reduction. *RSC Adv* 8:24819–24826. <https://doi.org/10.1039/c8ra04332a>
- Carmichael J, Degraff WG, Gazdar AF et al (1987) Evaluation of a Tetrazolium-based semiautomated colorimetric assay : assessment of chemosensitivity testing evaluation of a Tetrazolium-based semiautomated colourimetry assay: assessment. *Am Assoc Cancer Res* 47:936–942
- Chen T, Shi N, Afzali A (2019) Chemopreventive effects of strawberry and black raspberry on colorectal cancer in inflammatory bowel disease. *Nutrients* 11:1261. <https://doi.org/10.3390/nu11061261>
- Choudhary G (2012) Anti-ulcer activity of the ethanolic extract of *Terminalia bellerica* Roxb. *Int J Pharm Chem Sci* 1(4):1293
- Deb A, Choudhury G, Barua S, Das B (2016) Pharmacological activities of Baheda (*Terminalia bellerica*): a review. *J Pharm Phytochem* 5(1):194
- Devi P, Kaleeswari S, Poonkothai M (2014) Antimicrobial activity and phytochemical analysis of fruit extracts of *Terminalia bellerica*. *Int J Pharm Pharm Sci* 6(5):639–642
- Dharmaratne MPJ, Manoraj A, Thevanesam V et al (2018) *Terminalia bellerica* fruit extracts: in-vitro antibacterial activity against selected multidrug-resistant bacteria, radical scavenging activity and cytotoxicity study on BHK-21 cells. *BMC Complement Altern Med*. <https://doi.org/10.1186/s12906-018-2382-7>
- Fernandes AR, Mendonça-Martins I, Santos MFA et al (2020) Improving the anti-inflammatory response via gold nanoparticle vectorization of CO-releasing molecules. *ACS Biomater Sci Eng* 6:1090–1101. <https://doi.org/10.1021/acsbomaterials.9b01936>
- Gao W, Wang L, Wang K et al (2019a) Enhanced anti-inflammatory activity of peptide-gold nanoparticle hybrids upon cigarette smoke extract modification through TLR inhibition and autophagy induction. *ACS Appl Mater Interfaces* 11:32706–32719. <https://doi.org/10.1021/acscami.9b10536>
- Gao W, Wang Y, Xiong Y et al (2019b) Size-dependent anti-inflammatory activity of a peptide-gold nanoparticle hybrid in vitro and in a mouse model of acute lung injury. *Acta Biomater* 85:203–217. <https://doi.org/10.1016/j.actbio.2018.12.046>
- Habiba K, Aziz K, Sanders K et al (2019) Enhancing colorectal cancer radiation therapy efficacy using silver nanoprisms decorated with graphene as radiosensitizers. *Sci Rep* 9:1–9. <https://doi.org/10.1038/s41598-019-53706-0>
- Hainfeld JF, Slatkin DN, Focella TM, Smilowitz HM (2006) Gold nanoparticles: a new X-ray contrast agent. *Br J Radiol* 79:248–253. <https://doi.org/10.1259/bjr/13169882>
- Halliwell B, Gutteridge J (2015) *Free radicals in biology and medicine*. Oxford University Press, USA
- Hao M, Kong C, Jiang C et al (2019) Polydopamine-coated Au-Ag nanoparticle-guided photothermal colorectal cancer therapy through multiple cell death pathways. *Acta Biomater* 83:414–424. <https://doi.org/10.1016/j.actbio.2018.10.032>
- Hazra K (2019) phytochemical investigation of *Terminalia bellerica* fruit inside. *Asian J Pharm Clin Res* 12:191–194
- Huang BH, Zhuo JL, Leung CHW et al (2012) PRAP1 is a novel executor of p53-dependent mechanisms in cell survival after DNA damage. *Cell Death Dis* 3:e442. <https://doi.org/10.1038/cddis.2012.180>
- Kamal R, Chadha VD, Dhawan DK (2018) Physiological uptake and retention of radiolabeled resveratrol loaded gold nanoparticles (99mTc-Res-AuNP) in colon cancer tissue. *Nanomedicine Nanotechnology, Biol Med* 14:1059–1071. <https://doi.org/10.1016/j.nano.2018.01.008>
- Khan MA, Khan MJ (2018) Nano-gold displayed anti-inflammatory property via NF- κ B pathways by suppressing COX-2 activity. *Artif Cells, Nanomedicine, Biotechnol* 46:1149–1158. <https://doi.org/10.1080/21691401.2018.1446968>
- Khan A (2008). Pharmacodynamic evaluation of *Terminalia bellerica* for its antihypertensive effect. *J Food Drug Analysis* <https://doi.org/10.38212/2224-6614.2355>
- Kumar B, Divakar K, Tiwari P, Salhan M, Goli D (2010) Evaluation of the anti-diarrhoeal effect of aqueous and ethanolic extracts of fruit pulp of *Terminalia bellerica* in rats. *Int J Drug Develop Res* 2(4):769–779
- Kumari S, Kumari P, Panda PK et al (2019) Molecular aspect of phytofabrication of gold nanoparticle from *Andrographis peniculata* photosystem II and their in vivo biological effect on embryonic zebrafish (*Danio rerio*). *Environ Nanotechnol Monit Manag* 11:100201. <https://doi.org/10.1016/j.enmm.2018.100201>
- Latha D, Prabu P, Arulvasu C et al (2018) Enhanced cytotoxic effect on human lung carcinoma cell line (A549) by gold nanoparticles synthesised from *Justicia adhatoda* leaf extract. *Asian Pac J Trop Biomed* 8:540–547. <https://doi.org/10.4103/2221-1691.245969>
- Marill J, Mohamed Anesary N, Paris S (2019) DNA damage enhancement by radiotherapy-activated hafnium oxide nanoparticles improves cGAS-STING pathway activation in human colorectal cancer cells. *Radiother Oncol* 141:262–266. <https://doi.org/10.1016/j.radonc.2019.07.029>
- Namasivayam SKR, Venkatachalam G, Bharani RSA (2020) Immuno biocompatibility and anti-quorum sensing activities of chitosan-gum acacia gold nanocomposite (CS-GA-AuNC) against *Pseudomonas aeruginosa* drug-resistant pathogen. *Sustain Chem Pharm* 17:100300
- Owaid MN, Al-Saeedi SSS, Abed IA (2017) Biosynthesis of gold nanoparticles using yellow oyster mushroom *Pleurotus cornucopiae* var. *citrinopileatus*. *Environ Nanotechnol Monit Manag* 8:157–162. <https://doi.org/10.1016/j.enmm.2017.07.004>
- Peterson CT, Denniston K, Chopra D (2017) Therapeutic uses of Triphala in ayurvedic medicine. *J Altern Complement Med* 23:607–614. <https://doi.org/10.1089/acm.2017.0083>
- Rabel AM, Namasivayam SKR, Prasanna M, Bharani RSA (2019) A green chemistry to produce iron oxide—chitosan nanocomposite (CS-IONC) for the upgraded bio-restorative and pharmacotherapeutic activities-Supra molecular nanof ormulation against drug-resistant pathogens and malignant growth. *Int J Biol Macromol* 138:1109–1129. <https://doi.org/10.1016/j.ijbiomac.2019.07.158>
- Roshni K, Younis M, Ilakkiyapavai D, Basavaraju P, Puthamohan VM (2018) Anticancer activity of biosynthesized silver nanoparticles using *Murraya koenigii* leaf extract against HT-29 colon cancer cell line. *J Cancer Sci Ther* 10:072–075. <https://doi.org/10.4172/1948-5956.1000521>
- Saha PK, Patra PH, Pradhan R (2011) Effect of *Terminalia bellerica* & *Terminalia chebula* on wound healing in induced dermal wounds in Rabbits. *Pharmacol Online* 2:235–241
- Shang C, Cai C, Zhao C, Du Y (2018) Synthesis and anti-inflammatory activity of gold-nanoparticle bearing a dermatan sulfate

- disaccharide analog. *Chinese Chem Lett* 29:81–83. <https://doi.org/10.1016/j.ccllet.2017.06.010>
- Sharma US, Sharma K, Singh A et al (2010) Screening of Terminalia bellirica fruits extracts for its analgesic and antipyretic activities. *Jordan J Biol Sci* 3:121–124
- Shi M, Paquette B, Thippayamontri T et al (2016) Increased radiosensitivity of colorectal tumors with intra-tumoral injection of low dose of gold nanoparticles. *Int J Nanomedicine* 11:5323–5333. <https://doi.org/10.2147/IJN.S97541>
- Singh A (2017) Comparative therapeutic effects of plant-extract synthesized and traditionally synthesised gold nanoparticles on alcohol-induced inflammatory activity in SH-SY5Y cells in vitro. *Biomedicines* 5:70. <https://doi.org/10.3390/biomedicines5040070>
- Singh M, Harris-Birtill DCC, Markar SR et al (2015) Application of gold nanoparticles for gastrointestinal cancer theranostics: a systematic review. *Nanomed Nanotechnol Biol Med* 11:2083–2098
- Singh P, Ahn S, Kang J-P et al (2017) *In vitro* anti-inflammatory activity of spherical silver nanoparticles and monodisperse hexagonal gold nanoparticles by fruit extract of *Prunus serrulata*: a green synthetic approach. *Artif Cells, Nanomed, Biotechnol* 46:1–11. <https://doi.org/10.1080/21691401.2017.1408117>
- Uchide N, Tadera C, Sarai H et al (2006) Characterisation of monocyte differentiation-inducing (MDI) factors derived from human fetal membrane chorion cells undergoing apoptosis after influenza virus infection. *Int J Biochem Cell Biol* 38:1926–1938. <https://doi.org/10.1016/j.biocel.2006.05.014>
- Uchiyama MK, Deda DK, de Paula Rodrigues SF et al (2014) *In vivo* and *In vitro* toxicity and anti-inflammatory properties of gold nanoparticle bioconjugates to the vascular system. *Toxicol Sci* 142:497–507. <https://doi.org/10.1093/toxsci/kfu202>
- Wang R, Huang J, Chen J et al (2019a) Enhanced anti-colon cancer efficacy of 5-fluorouracil by epigallocatechin-3-gallate co-loaded in wheat germ agglutinin-conjugated nanoparticles. *Nanomed Nanotechnol Biol Med* 21:102068. <https://doi.org/10.1016/j.nano.2019.102068>
- Wang T, Wang F, Sun M et al (2019b) Gastric environment-stable oral nanocarriers for in situ colorectal cancer therapy. *Int J Biol Macromol* 139:1035–1045. <https://doi.org/10.1016/j.ijbiomac.2019.08.088>
- Yang H, Kozicky L, Saferali A et al (2016) Endosomal pH modulation by peptide-gold nanoparticle hybrids enables potent anti-inflammatory activity in phagocytic immune cells. *Biomaterials* 111:90–102. <https://doi.org/10.1016/j.biomaterials.2016.09.032>
- Yuan YG, Peng QL, Ggurunathan S (2017) Silver nanoparticles enhance the apoptotic potential of gemcitabine in human ovarian cancer cells: combination therapy for effective cancer treatment. *Int J Nanomedicine* 12:6487–6502. <https://doi.org/10.2147/IJN.S135482>
- Zhang P, Darmon A, Marill J et al (2020) Radiotherapy-activated hafnium oxide nanoparticles produce abscopal effect in a mouse colorectal cancer model. *Int J Nanomedicine* 15:3843–3850. <https://doi.org/10.2147/IJN.S250490>
- Zhong Y, Su T, Shi Q et al (2019) Co-administration of iRGD enhances tumour-targeted delivery and antitumor effects of paclitaxel-loaded PLGA nanoparticles for colorectal cancer treatment. *Int J Nanomedicine* 14:8543–8560. <https://doi.org/10.2147/IJN.S219820>

Authors and Affiliations

S. Karthick Raja Namasivayam¹  · Gayathri Venkatachalam¹ · R. S. Arvind Bharani¹ · J. Aravind Kumar² · S. Sivasubramanian³

¹ Centre for Bioresource Research & Development (C-BIRD), Department of Biotechnology, Sathyabama Institute of Science and Technology, Chennai, Tamil Nadu 600119, India

² Department of Chemical Engineering, Sathyabama Institute of Science and Technology, Chennai, Tamil Nadu 600119, India

³ Department of Chemical Engineering, Higher College of Technology, Muscat, Oman